Disruption of superficial white matter in the emotion regulation network in bipolar disorder

Shufei Zhang[a,1], Ying Wang[b,c,**,1], Feng Deng[a], Shuming Zhong[d], Lixiang Chen[a], Xiaomei Luo[b,c], Shaojuan Qiu[b,c], Ping Chen[a], Guanmao Chen[b,c], Huiqing Hu[a], Sunkai Lai[d], Huiyuan Huang[a], Yanbin Jia[d], Li Huang[b,c], Ruiwang Huang[a,*]

[a] Center for the Study of Applied Psychology, Key Laboratory of Mental Health and Cognitive Science of Guangdong Province, School of Psychology, Institute for Brain Research and Rehabilitation, South China Normal University, Guangzhou 510631, PR China
[b] Institute of Molecular and Functional Imaging, Jinan University, Guangzhou 510630, China
[c] Medical Imaging Center, First Affiliated Hospital of Jinan University, Guangzhou 510630, China
[d] Department of Psychiatry, First Affiliated Hospital of Jinan University, Guangzhou 510630, China

ARTICLE INFO

ABSTRACT

Bipolar disorder (BD) is characterized by emotion dysregulation and involves changes in the gray matter (GM) and white matter (WM). Although previous diffusion tensor imaging (DTI) studies reported changes in the diffusion properties of the deep WM (DWM) in BD patients, the diffusion properties of the superficial WM (SWM) are rarely investigated. In this study, we tried to determine whether the diffusion parameters of the SWM were altered in BD patients compared to controls and whether the changes were associated with the disrupted emotion regulation of the BD patients. We collected DTI data from 37 BD patients and 42 gender- and age-matched healthy controls (HC). Using probabilistic tractography, we defined a population-based SWM mask based on all the subjects. After performing the tract-based spatial statistical (TBSS) analyses, we identified the SWM areas in which the BD patients differed from the controls. This study showed significantly reduced fractional anisotropy in the SWM (FA_{SWM}) in the BD patients compared to the HC in the bilateral dorsolateral prefrontal cortex (dlPFC), ventrolateral prefrontal cortex (vlPFC), medial prefrontal cortex (mPFC), and the left parietal cortex. Moreover, compared to the controls, the BD patients showed significantly increased mean diffusivity (MD_{SWM}) and radial diffusivity (RD_{SWM}) in the SWM in the right frontal cortex. This study presents altered cortico-cortical connections proximal to the regions related to the emotion dysregulation of BD patients, which indicated that the SWM may serve as the brain's structural basis underlying the disrupted emotion regulation of BD patients. The disrupted FA_{SWM} in the parietal cortex may indicate that the emotion dysregulation in BD patients is related to the cognitive control network.

1. Introduction

Bipolar disorder (BD) (Chang et al., 2013) is characterized by dysfunction in emotion regulation (Phillips and Swartz, 2014), which refers to the ability of an individual to modulate their response to emotional stimuli (Frank et al., 2014). Dysregulation of the emotions may lead to mood disorders (Townsend et al., 2013). Previous studies revealed a neural circuit (Phillips and Swartz, 2014; Phillips et al., 2008), comprising cortical regions that include the ventrolateral prefrontal cortex (vlPFC), dorsolateral prefrontal cortex (dlPFC), and medial prefrontal cortex (mPFC) as well as subcortical regions, including the amygdala and striatum, which may underlie disrupted emotion

regulation in BD patients. Recent meta-analyses (Zilverstand et al., n.d.; Buhle et al., 2014) that summarized previous studies of emotion regulation suggested that this emotion regulatory network largely overlaps with the cognitive control network and indicated that abnormalities in the parietal regions, especially in the inferior parietal (IP) and superior parietal (SP) gyrus, may also indicate a deficit in emotion regulation.

Although the pathology of BD remains unknown, white matter (WM) abnormality is believed to be related to the disease mechanism (Mahon et al., 2010). Brain WM can be classified into two systems, the superficial WM (SWM) and the deep WM (DWM), based on differences in their morphological features, including size, arrangement, and distribution (Oishi et al., 2008). WM studies in BD have primarily considered the DWM, which comprises large WM bundles and enables long-range connections between gray matter (GM) regions. In contrast, the SWM enables local connections between cortico-cortical regions. The SWM is located below the cortex (Oishi et al., 2008) and consists of short cortico-cortical fibers, such as U-shaped and intra-lobar fibers (Nazeri et al., 2013).

Although less is known about the specific functions of the SWM, several studies have indicated that the SWM is related to human cognitive functions. For example, Nazeri et al. found that the SWM contributes to cognitive performance in patients with schizophrenia (Nazeri et al., 2013) and in aging populations (Nazeri et al., 2015). Recently, Liu et al. (Liu et al., 2016) reported that in temporal lobe epilepsy the SWM serves as an important link between the functional and structural networks. These findings suggest an important role for the SWM, but an effective tractography for SWM fibers has not yet been fully identified.

Because of the complexity of the brain's cortical folding patterns (Chen et al., 2013; Nie et al., 2012), compared to the DWM, the SWM is more complex, which impede reconstructing long-range connections near the cortical regions (Reveley et al., 2015) using tractography. For example, the fractional anisotropy (FA) and curvature measured at the white/gray matter boundary (WGB) are respectively lower and sharper than those measured in the DWM. Additionally, in a given fiber bundle, it is difficult to distinguish between the fibers (Nazeri et al., 2013) that belong to the DWM and those that belong to the SWM. However, with more advanced fiber-tracking algorithms (Behrens et al., 2007), researcher can use "waypoint mask" or "exclusion mask" to constrain fibers to those near the cortex and remove the long-range fibers passing through the exclusion regions, if the seeds were selected at the WGB.

In this study, our goals were to determine whether the SWM is altered in BD patients compared to healthy controls (HC) and to determine whether these SWM alterations are associated with the disrupted emotion regulation of BD patients. In the calculations, we adopted probabilistic tractography (Behrens et al., 2007) to reconstruct a population-based SWM mask and used a tract-based spatial statistics (TBSS) (Smith et al., 2006) analysis to assess the differences of diffusion parameters in the SWM regions between the BD patients and the HC group.

2. Methods

2.1. Subjects

Thirty-seven BD subjects were recruited from the First Affiliated Hospital of Jinan University (AHJU), Guangzhou. The eligible subjects for this study were right-handed, aged 18–55 years old, and able to read and write. All the patients (26 M/11 F, aged 18–51 years old) completed the Young Mania Rating Scale (YMRS) (Young et al., 1978) and the Hamilton Depression Scale (HAMD) (Whisman et al., 1989). The YMRS was used to measure the manic degree of the BD patients in the week before the scan and the HAMD was used to detect each individual's depression state. The inclusion criteria for the BD group were (i) no long-term history of medication usage and (ii) a YMRS score < 12 and HAMD score > 21. The exclusion criteria for the patients were as

Table 1
Demographic characteristics of the patients with bipolar disorder (BD) and the healthy controls (HC).

Parameter	BD ($n = 37$)	HC ($n = 42$)	p-value (two-tailed)
Gender	26 M/11 F	26 M/16 F	0.483[a]
Age (years old)	26.3 ± 8.5	27.6 ± 9.0	0.515[b]
Education level (years)	13.7 ± 2.3	15.3 ± 2.5	0.004[**],[c]
Disease exacerbations (times)	3.0 ± 1.9	N/A	
Onset age (years old)	21.7 ± 10.6	N/A	
Duration time (months)	49.6 ± 61.4	N/A	
HAMD	28.8 ± 6.0	N/A	
YMRS	3.0 ± 2.9	N/A	

Abbreviations: HAMD, Hamilton Depression Scale; YMRS, Young Mania Rating Scale.
[a] The p-value was obtained from a χ^2-test.
[b] The p-value was obtained from a two-sample t-test.
[c] The p-value was obtained from a two-sample t-test.
[**] p-value < .01.

follows: patients with other comorbid DSM-IV Axis-I psychiatric disorders or a history of neurological disorders, organic brain disorders, cardiovascular diseases, pregnancy, and alcohol or substance abuse. We also recruited forty-two healthy subjects (26 M/16 F, aged 18–52 years old) as the control group in the hospital. The exclusion criteria for the HC were same as that of the BD patients. In addition, to remove co-morbidities we excluded subjects who had a history of or first-degree relatives with psychiatric illness. Table 1 lists the demographic characteristics of the BD patients and the HC group and the clinical performance of the BD patients. This study was approved by the Institutional Review Board of the First Affiliated Hospital of Jinan. Written informed consent was obtained from each subject prior to the study.

2.2. Data acquisition

All MRI data were acquired on a 3 T GE MR750 scanner with 8-channel head coil. The DTI data were obtained using a single-shot diffusion-weighted EPI sequence with the following parameters: repetition time (TR) = 8, 000 ms, echo time (TE) = 68 ms, field of view (FOV) = 256 mm × 256 mm, data matrix = 128 × 128, voxel size = 2 × 2 × 2 mm³, slice thickness = 2 mm, flip angle (FA) = 90°, 30 diffusion-sensitive directions with $b = 1, 000$ mm²/s, 5 volumes with $b = 0$ mm²/s, and 75 slices without inter-slice gap. All the DTI data were scanned twice to improve the signal-to-noise ratio (SNR). In addition, we acquired high resolution brain structural images with a T1-weighted 3D Ax FSPGR BRAVO sequence (TR = 8.212 ms, TE = 3.22 ms, inversion time = 450 ms, FA = 12°, data matrix = 256 × 256, FOV = 256 mm × 256 mm, voxel size = 1 × 1 × 1 mm³, slice thickness = 1 mm, and 136 axial slices covering the whole brain).

3. Data processing

3.1. Image preprocessing

DTI data preprocessing was performed in FDT, a tool implemented in FSL (http://fsl.fmrib.ox.ac.uk/fsl). First, for each subject, the two repeated DTI datasets were concatenated and averaged. Second, non-diffusion-weighted images (b_0) were extracted and non-brain tissues were removed using FSL/bet. Third, head-motion and eddy current-induced distortions were corrected using FSL/eddy_correct, and gradient orientations of the B-matrix were rotated (Leemans and Jones, 2009). Then, the eigenvalues of diffusion tensor were estimated using FSL/dtifit, and fractional anisotropy (FA), radial diffusivity (RD), axonal diffusivity (AD), and mean diffusivity (MD) were generated. Finally, a 2-tensor model was fitted at each voxel for necessary

Fig. 1. Overview of the pipeline for the tract-based spatial statistics (TBSS) on the superficial white matter (SWM). a) Seed mask. The seed mask (red) was initially extracted from T1w images and registered to individual FA images by affine transformations (dof 12). b) Exclusion mask. The exclusion mask (blue) was created by registering the JHU-DTI-81 white matter (WM) atlas to individual FA images by the inverse TBSS registration. c) SWM mask. Individual tractography results were registered to the FMRIB58_FA template by the TBSS registration and then averaged across subjects as a population-based map. The SWM mask was created by applying a threshold of 0.5 to the population-based map. d) TBSS. Individual FA images were registered to the FMRIB58_FA template by the TBSS registration. The SWM skeleton (green) was only reconstructed in the SWM defined regions.

preparation for the probabilistic tractography using FSL/bedpostx.

The structural images were preprocessed using an automatic pipeline called "recon-all" in FreeSurfer (http://surfer.nmr.mgh.harvard.edu/). The pipeline involved the following steps: 1) motion correction and intensity normalization, 2) brain extraction, 3) segmentation of WM, gray matter (GM), and cerebrospinal fluid (CSF), and 4) WGB and pial surface generation.

3.2. TBSS analyses on the SWM

Fig. 1 illustrates the pipeline for TBSS analyses on the SWM. The steps were as follows: a) Seeds mask creation. Individual WGB mask was extracted from the WM/GM interface surface from the FreeSurfer and transformed to the diffusion space using the affine transformation (dof = 12) as the seed mask of each subject (Fig. 1a). b) Exclusion mask creation. FA images of all subjects were initially registered to the FMRIB58_FA template in the MNI space by using the TBSS non-linear transformation. Then the Johns Hopkins University ICBM-DTI-81 white-matter labels atlas (Wakana et al., 2007) was transformed into individual diffusion space using the inverse TBSS non-linear transformation as the exclusion mask for each subject (Fig. 1b). c) SWM mask reconstruction. We generated probabilistic streamlines, which were sampled distributions of voxel-wise principal diffusion directions, using FSL/protrackx. After the probabilistic tractography, each individual tractographic result was normalized by dividing by the total number of

the streamlines and then thresholded at 0.01% (Nazeri et al., 2015) to remove across-subjects variations. All the normalized SWM fibers were then non-linearly registered to MNI space using the TBSS non-linear transformation. We averaged the registered SWM masks across the subjects and created a probabilistic map for a population-based SWM map. Because of the inter-subject variability, we adopted a threshold of 50% (Nazeri et al., 2015) to create the SWM mask (Fig. 1c). d) TBSS analyses. The FA images for all subjects were aligned to the FMRIB58_FA template using the non-linear registration in FSL/fnirt. The non-linear transformation from individual diffusion space to MNI space was generated, and we inverted the transformation to create individual exclusion masks. Next, the registered FA images were averaged to create whole-brain mean FA images. To limit the TBSS on the SWM region, the mean FA images were multiplied by the SWM mask to create the mean FA_{SWM} images, and a skeleton procedure was applied to the mean FA_{SWM} images to reconstruct the FA_{SWM} skeleton, which is representative of SWM tracts with a line of common center. To remove non-WM tissues and false-positive fibers from the probabilistic results, we applied a threshold of FA > 0.2 to the FA_{SWM} skeleton. Then individual FA images were projected onto the FA_{SWM} skeleton (Fig. 1d). To provide more information about the diffusion properties of the SWM, we also considered the MD_{SWM}, RD_{SWM}, and AD_{SWM}, by projecting them onto the FA_{SWM} skeleton using a non-linear transformation.

3.3. Statistics

3.3.1. Demographic statistics

All the demographic statistics were calculated using SPSS 19.0. We used two-sample t-tests to evaluate differences in age and education level between the two groups. For the gender factor, we used the χ^2-test to calculate the group difference in gender. The statistical significance level for each test was set at $p < 0.05$ (two-tailed).

3.3.2. TBSS analyses

The calculation steps were as follows. (i) A general linear model (GLM) was applied to assess difference in FA_{SWM} between groups using a non-parametric permutation test (5000 permutations) (Winkler et al., 2014). In this study, because the demographic factors of the BD patients were not perfectly matched with those of the HC group, we took gender, age, and education level as covariates when testing the FA_{SWM} difference between groups. We also assessed the between-group differences in the mean diffusivity (MD_{SWM}), axonal diffusivity (AD_{SWM}), and radial diffusivity (RD_{SWM}) in the SWM by using the statistical method same to that of the FA_{SWM} analysis. The significance level was set at $p < 0.05$, which was corrected by a family-wise error (FWE) rate method. The clusters, which were corrected by a threshold-free cluster enhancement (TFCE) method (Smith and Nichols, 2009), were reported according to the LNAO-SWM79 atlas (Guevara et al., 2017). The LNAO-SWM79 atlas was adopted to determine the SWM bundles using deterministic tractography based on Desikan-Killiany parcellation. From the overlapping regions between the clusters and the atlas, we could determine the SWM bundles and associated cortical regions that showing significant between-group differences in FA_{SWM}, MD_{SWM}, RD_{SWM}, and AD_{SWM}.

3.3.3. Relationship between diffusion properties and clinical variables

In order to detect the relationship between diffusion properties and clinical variables of the BD patients, we first extracted the mean values of the FA_{SWM}, MD_{SWM}, AD_{SWM}, and RD_{SWM} in the clusters showing significant differences between groups, and then calculated the correlation between each of them and disease exacerbations, onset age, duration time of the BD patients. In the calculations, we also took gender, age, and educational level as covariates, and set the significance level at $p < 0.05$.

4. Results

4.1. Demographics

Table 1 lists demographic factors for each group and the clinical performance of the BD patients in this study. No significant difference was observed in either gender or age between the BD patients and the HC group ($p > .05$). A significant difference in education level was found between the two groups ($p < 0.01$).

4.2. Permutation results for the SWM

TBSS analyses showed no significant difference in AD_{SWM} between the BD group and the HC group, but we found significant between-group differences in FA_{SWM}, RD_{SWM}, and MD_{SWM} (Table 2). We found that compared to the HC group, the BD patients exhibited significantly uniformly reduced FA_{SWM} in five clusters (Fig. 2), which were labelled as Cluster-5, Cluster-4, Cluster-3, Cluster-2, and Cluster-1 from the largest to the smallest volume. According to the LNAO-SWM79 atlas, we determined the associated cortical regions and SWM bundles of these clusters (Fig. 3). We found that Cluster-5 is mainly distributed in the left prefrontal regions and located in the PoC-PrC, Op-PrC, RMF-SF, LOF-RMF, CMF-Op, Op-SF, CMF-RMF, Tr-SF, RAC-SF, and CMF-PrC bundles. Cluster-4 is distributed in the left fronto-parietal regions and located in the PoC-PrC bundles. Cluster-3 is distributed in the right prefrontal regions and located in the RMF-SF, Op-SF, and Tr-SF bundles.

Cluster-2 is distributed in the left parietal regions, and located in the IP-SP and SP-SM bundles. Cluster-1 is distributed in the right prefrontal regions, and located in the RMF-SF and RAC-SF bundles. We also found significantly increased RD_{SWM} and MD_{SWM} in the BD patients compared to the HC (Fig. 4). Similar to the labelling method of FA_{SWM} clusters, we found the two clusters with significant increased MD_{SWM} are distributed in the right frontal regions. The MD_{SWM} Cluster-1 is located in the CMF-PrC and Op-PrC bundles, and the MD_{SWM} Cluster-2 is located in the CMF-SF and CMF-PrC bundles. As for RD_{SWM}, the cluster with significantly increased RD_{SWM} is distributed in the right prefrontal cortex and is located in the RMF-SF and Tr-SF bundles.

4.3. Relationship between diffusion properties and clinical variables

The correlation analyses showed that there was no significant correlation between RD_{SWM}/MD_{SWM} and clinical variables of the BD patients. We found the FA_{SWM} between the vlPFC and the dlPFC (Cluster-3) correlated negatively with the disease exacerbations of the BD patients (Fig. 5).

5. Discussion

This study focused on SWM changes in patients with BD. We used an automatic probabilistic tractography approach to restrict the fibers near the cortex and discard the fibers passing through the exclusion regions. In this study, the BD patients showed an abnormally reduced FA_{SWM} around nodes in the dlPFC, vlPFC, mPFC, and parietal regions, indicating disrupted connections within the emotion regulatory network of the BD patients.

5.1. FA_{SWM} in the dlPFC

In the dlPFC, the BD patients showed reduced FA_{SWM} in the bilateral RMF-SF and the left CMF-RMF bundles compared to the HC group. The dlPFC is believed to be involved in working memory (Wager and Smith, 2003; Curtis, 2006), planning (Rosenbloom et al., 2012), and attention control (Hopfinger et al., 2000). In the emotion regulatory network, the dlPFC is assumed to be responsible for manipulating cognitive appraisals (Zilverstand et al., n.d.; Buhle et al., 2014). Previous studies (Frank et al., 2014; Eippert et al., 2007) have reported increased activation in the SF and middle frontal (MF) regions during emotion downregulation, findings which suggest that the dlPFC plays an important role in emotion regulation. Moreover, several studies (Townsend et al., 2013; Townsend and Altshuler, 2012) reported that BD patients showed reduced activation in the dlPFC compared to HC groups when the subjects downregulated their emotions. The abnormal activation in the dlPFC may be related to emotion dysregulation in BD patients. In this study, reduced FA_{SWM} in the bundles within the dlPFC, indicating disrupted cortico-cortical connections within the dlPFC, may reflect the abnormal emotion regulation of BD patients.

5.2. FA_{SWM} between the LOF and the dlPFC

In this study, the BD patients showed reduced FA_{SWM} in the left LOF-RMF bundle compared to the HC group. Previous studies suggested that LOF activation may be related to different responses to punishments (Kringelbach and Rolls, 2004) or to value expectations (Bermpohl et al., 2010). For example, BD patients exhibited increased activation under an increasing gain expectation and decreased activation under an increasing loss expectation, but the controls had an inverse activation in the LOF (Bermpohl et al., 2010). This inverse activation in the LOF between BD patients and controls under loss- or gain-expectation conditions may indicate that BD patients underestimate the punishments that may result from their behaviors. In this study, reduced FA_{SWM} in the bundles between the LOF and RMF, indicating altered connections around the LOF, may reflect abnormality in the LOF in BD patients.

Table 2
Clusters showing significant differences between the patients with bipolar disorder (BD) and the healthy controls (HC).

Cluster	MNI peak coordinates			Cluster size (mm³)	Mean value		p-value[a]	Hemi-sphere	Associated regions[b]
	x	y	z		BD	HC			
FA_{SWM}									
Cluster-1	19	49	17	41	0.40	0.43	0.04	R	RMF, SF, RAC
Cluster-2	−28	−52	35	118	0.34	0.37	0.028	L	IP, SP, SM
Cluster-3	19	25	36	158	0.49	0.52	0.002	R	RMF, Op, Tr, SF
Cluster-4	−34	−27	44	176	0.42	0.44	0.028	L	PoC, PrC
Cluster-5	−19	13	43	1, 173	0.42	0.44	0.012	L	PoC, PrC, Op, Tr, RMF, CMF, LOF, SF, RAC
MD_{SWM}									
Cluster−1	48	-1	36	50	7.6×10^{-4}	7.3×10^{-4}	0.038	R	CMF, Op, PrC
Cluster−2	36	-2	40	60	7.4×10^{-4}	7.2×10^{-4}	0.045	R	CMF, SF, PrC
RD_{SWM}									
Cluster-1	20	50	11	86	5.9×10^{-4}	5.7×10^{-4}	0.035	R	RMF, Tr, SF

Abbreviations: RMF, rostral middle frontal gyrus; SF, superior frontal gyrus; RAC, rostral anterior cingulate gyrus; IP, inferior parietal gyrus; SP, superior parietal gyrus; SM, supramarginal gyrus; Op, pars opercularis gyrus; Tr, pars triangularis gyrus; PoC, postcentral gyrus; PrC, precentral gyrus; CMF, caudal middle frontal gyrus; LOF, lateral orbitofrontal gyrus; L (R): left (right)-hemisphere. All the abbreviations were defined based on the Desikan-Killiany atlas. $FA_{SWM}/MD_{SWM}/RD_{SWM}$, fractional anisotropy/mean diffusivity/radial diffusivity in the superficial white matter.

  [a] The p-value of the cluster-based peak coordinates under *FWE* correction.
  [b] The cortical regions connected by SWM bundles with reduced FA_{SWM} were obtained from the tract-based spatial analysis (TBSS). These regions were determined according to the LNAO-SWM79 atlas.

5.3. FA_{SWM} between the vlPFC and the dlPFC

In this study, compared to the HC group, the BD patients showed reduced FA_{SWM} in the bilateral Op-SF, Tr-SF, and left CMF-Op bundles, passing from the dlPFC to the vlPFC. The vlPFC and the dlPFC are highly interconnected (Goulas et al., 2012) in the human brain, and the vlPFC was found to play an inhibitory role in cognitive, motor, and affective responses in the emotion regulation network (Berkman et al.,
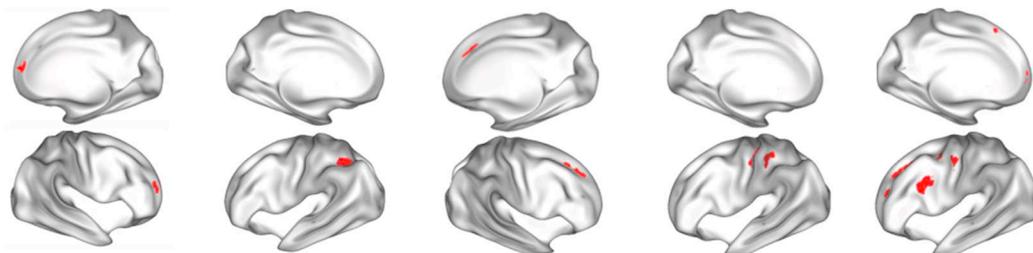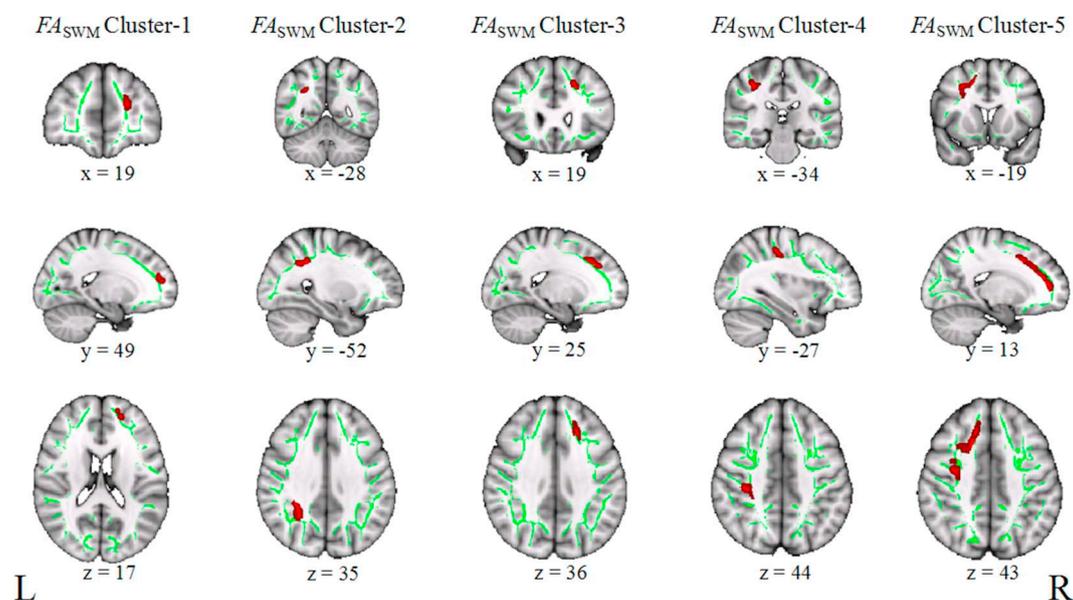
Fig. 2. Presentations of the tract-based spatial statistics (TBSS) results in FA_{SWM}. a) Surface-based representation. The five clusters showing reduced FA_{SWM} in the patients with bipolar disorder (BD) compared to the controls were projected on an inflated surface. b) Volumetric representation. The five clusters were displayed with three-dimensional view at their peak MNI coordinates. L, left hemisphere; R, right hemisphere. FA_{SWM}, fractional anisotropy in the superficial white matter.
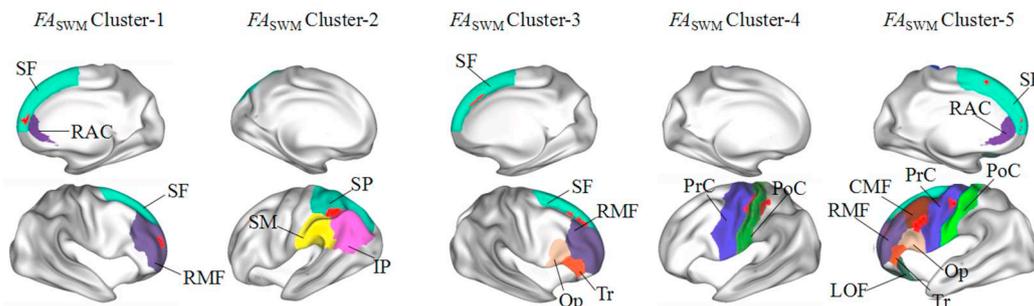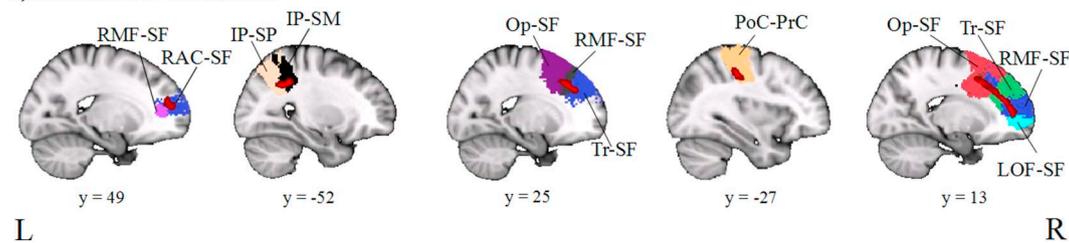
Fig. 3. Presentations of associated cortical regions and superficial white matter (SWM) bundles with significantly reduced FA_{SWM} in patients with bipolar disorder (BD) compared to controls. a) shows the associated cortical regions, which were connected by disrupted SWM bundles. b) shows the associated SWM bundles with significantly reduced FA_{SWM}. FA_{SWM}, fractional anisotropy in the superficial white matter. SF, superior frontal gyrus; RAC, rostral anterior cingulate gyrus; RMF, rostral middle frontal gyrus; CMF, caudal middle frontal gyrus; IP, inferior parietal gyrus; SP, superior parietal gyrus; SM, supramarginal gyrus; Op, pars opercularis gyrus; Tr, pars triangularis; PoC, postcentral gyrus; PrC, precentral gyrus; LOF, lateral orbitofrontal gyrus.
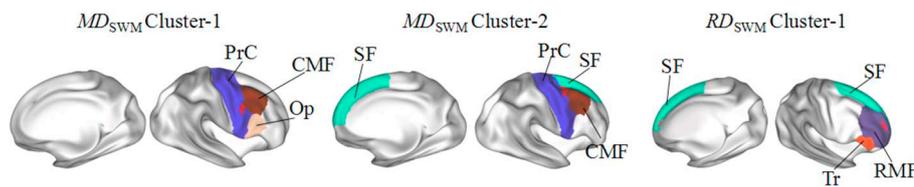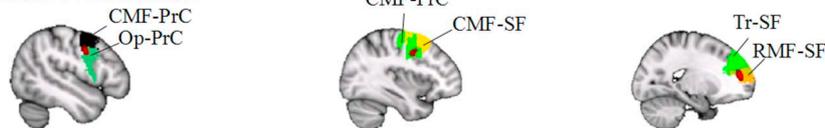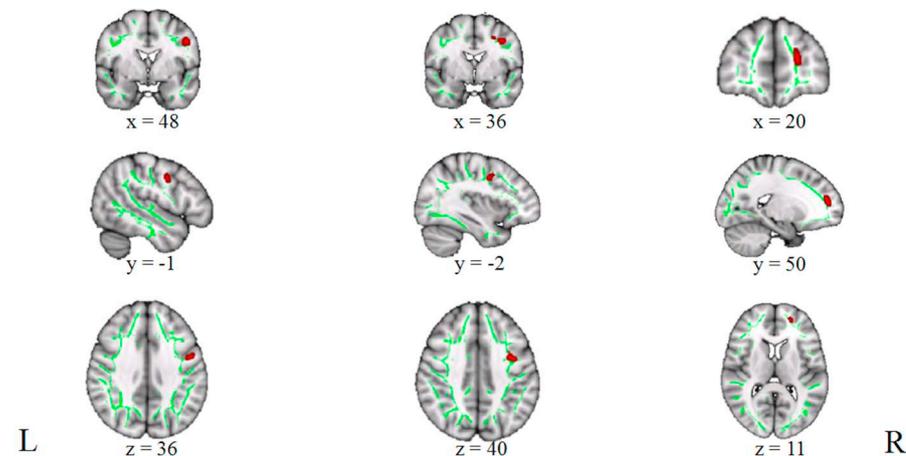
Fig. 4. Presentations of the tract-based spatial statistics (TBSS) results in MD_{SWM} and RD_{SWM}. a) shows the cortical regions, which were connected by the disrupted SWM bundles. b) shows the SWM bundles with significantly changed MD_{SWM} or RD_{SWM}, separately. c) displays the clusters showing significantly changed RD_{SWM} or MD_{SWM} with three-dimensional view at their peak MNI coordinates. L, left hemisphere; R, right hemisphere. RD_{SWM}/MD_{SWM}, radial diffusivity/mean diffusivity in the superficial white matter. PrC, precentral gyrus; CMF, caudal middle frontal gyrus; RMF, rostral middle frontal gyrus; Op, pars opercularis gyrus; SF, superior frontal gyrus; Tr, pars triangularis.
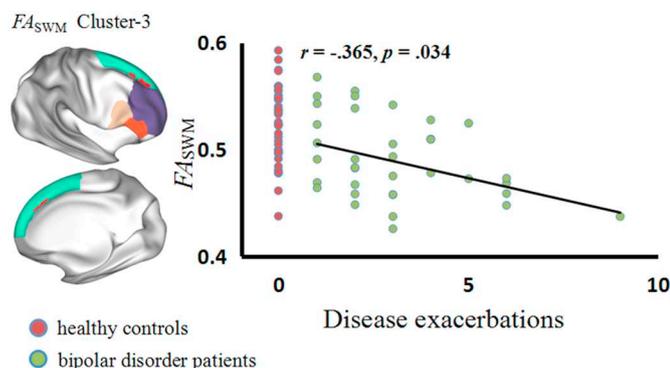
Fig. 5. Correlation between FA_{SWM} and disease exacerbations of the patients with bipolar disorder (BD). In the scatter diagram, the green dot represents the BD patients and the red dot represents the controls. FA_{SWM}, fractional anisotropy in the superficial white matter.

2009). Townsend et al. (Townsend et al., 2013) reported that BD patients showed reduced activation in the vlPFC and the dlPFC compared to a HC group when the subjects downregulated their emotions. Zilverstand et al. (Zilverstand et al., n.d.) reported reduced recruitment of the dlPFC and the vlPFC in BD patients compared to a control group, under emotion downregulating conditions. Moreover, Morawetz et al. (Morawetz et al., 2016) found that connections between the dlPFC and the vlPFC mediated the regulatory process of individual emotions. In this study, reduced FA_{SWM} between the dlPFC and the vlPFC, indicating abnormal connections between the dlPFC and the vlPFC, may influence the emotion regulatory process in the emotions of BD patients.

5.4. FA_{SWM} between the RAC and dlPFC

In this study, the BD patients showed reduced FA_{SWM} in the bilateral RAC-SF bundles, which connect the rostral part of the anterior cingulate cortex (RAC) and the dlPFC, compared to the HC group. The RAC is believed to be involved in affective functioning (Bush et al., 2000). Matsuo et al. (Matsuo et al., 2009) found that the RAC volume was negatively correlated with impulsivity in BD patients. Several studies (Wagner et al., 2006; Matsuo et al., 2007) involving attention and working memory tasks have reported that patients with major depression disorder (MDD) showed increased activation in the RAC compared to controls, compensating for the dlPFC, to meet task demands. For example, Wagner et al. (Wagner et al., 2006) reported that during Stroop tasks MDD patients showed highly positive correlations between activity in the dlPFC, the RAC, and interference scores, but the controls showed no significant correlations between these. Treadway et al. (Treadway et al., 2009) suggested that this positive correlation in MDD patients may reflect cortical inefficiency between the RAC and the dlPFC. In this study, the reduced FA_{SWM}, showing a weak connection between the RAC and the dlPFC, may reflect cortical inefficiency between the RAC and the dlPFC in BD patients.

5.5. FA_{SWM} in the fronto-parietal regions

In this study, the BD patients showed reduced FA_{SWM} in the bundles in the left IP-SP, SP-SM, and PoC-PrC, compared to the HC group. Niendam et al. (Niendam et al., 2012) found that the parietal cortex is involved in the cognitive control network and that the IP and SP are activated as well as the dlPFC in inhibition or in working memory tasks. Recent meta-analyses (Zilverstand et al., n.d.; Buhle et al., 2014) revealed that the emotion regulatory network largely overlaps with the cognitive control network, in which the IP and SP are involved in allocating attention and salience detection (Corbetta and Shulman, 2002). Picó-Pérez et al. (Picó-Pérez et al., 2017) reported an aberrant activation in mood and anxiety disorder patients, who displayed

increased activation in the SM, SP, and PrC but reduced activation in the vlPFC, mPFC, and posterior cingulate cortex (PCC) compared to a control group while regulating negative emotions. This increased activation in the SM, SP, and PrC may indicate a compensatory mechanism for impaired cortical control of negative emotions in the patients. In this study, reduced FA_{SWM} around the IP, SP, and SM, showing the abnormal connections around them, may reflect abnormality in nodes of the cognitive control network in BD patients.

In addition, we found reduced FA_{SWM} in the PoC-PrC, Op-PrC, and CMF-PrC bundles in the left hemisphere. Although the PoC and PrC are in the somatosensory and motor region, they have been found to be important in discriminating emotions (Saarimäki et al., 2016). Kujawa et al. (Kujawa et al., 2015) found that activation in the PrC and PoC when responding to threatening faces better predicted the treatment response in adult anxiety disorder patients, suggesting an important role for the PrC and PoC in emotion regulation. In this study, reduced FA_{SWM}, showing abnormal connections around the PoC and PrC, may reflect abnormality in PrC and PoC was related to disrupted emotion regulation of BD patients.

5.6. Relationship between FA_{SWM} and disease exacerbations

This study showed that FA_{SWM} of the Cluster-3 exhibited negative correlation with disease exacerbations of the BD patients. Cluster-3 comprised the right RMF-SF, Op-SF, and Tr-SF bundles passing from the vlPFC to the dlPFC. Townsend et al. (Townsend and Altshuler, 2012) indicated that dysfunction in the vlPFC may result in emotion dysregulation and make BD patients susceptible to relapse into the manic state. The connection between the dlPFC and vlPFC was found to mediate the emotion regulatory process (Morawetz et al., 2016). Thus, reduced FA_{SWM} indicating a weak connection between the vlPFC and the dlPFC, may influence the emotion regulatory process and make BD patients more susceptible to the manic state.

5.7. Limitations

Several limitations in this study should be addressed. First, the main limitation arises from the sample size of the BD patients ($n = 37$), which may preclude the validation of its inferences with respect to other clinical populations with BD. Second, specific scales for measuring the emotion regulatory ability of BD patients were not used; we only utilized the HAMD and YMRS scales. Thus, the relationship between the emotion regulatory ability of BD patients and diffusion properties in the SWM could not be detected in this study. Third, this study primarily analyzed DTI data without a functional MRI data analysis, so we could not provide study-specific relationships between brain structure and function. Further SWM studies in BD patients should consider using multi-modal data. Fourth, the goal of this study was to detect SWM differences in the BD patients compared to the HC, so we did not consider the subcortical regions, which are known to be very important in the emotion regulatory network.

6. Conclusion

In conclusion, this study presents altered cortico-cortical connections near the regions related to emotion dysregulation in BD patients. The findings indicated that the SWM may serve as the brain structural basis underlying the disrupted emotion regulation of BD patients. In contrast with the emotion regulatory network, the disrupted FA_{SWM} in the parietal cortex may indicate that emotion dysregulation in BD patients is related to the cognitive control network.

Competing interests statement

The authors declare that they have no competing financial interests.

References

Behrens, T.E., et al., 2007. Probabilistic diffusion tractography with multiple fibre orientations: what can we gain? NeuroImage 34 (1), 144–155.

Berkman, E.T., Burklund, L., Lieberman, M.D., 2009. Inhibitory spillover: Intentional motor inhibition produces incidental limbic inhibition via right inferior frontal cortex. NeuroImage 47 (2), 705.

Bermpohl, F., et al., 2010. Altered representation of expected value in the orbitofrontal cortex in mania. Hum. Brain Mapp. 31 (7), 958–969.

Buhle, J.T., et al., 2014. Cognitive reappraisal of emotion: a meta-analysis of human neuroimaging studies. Cereb. Cortex 24 (11), 2981.

Bush, G., Luu, P., Posner, M.I., 2000. Cognitive and emotional influences in anterior cingulate cortex. Trends Cogn. Sci. 4 (6), 215.

Chang, S.H., et al., 2013. BDgene: a genetic database for bipolar disorder and its overlap with schizophrenia and major depressive disorder. Biol. Psychiatry 74 (10), 727–733.

Chen, H., et al., 2013. Coevolution of gyral folding and structural connection patterns in primate brains. Cereb. Cortex 23 (5), 1208–1217.

Corbetta, M., Shulman, G.L., 2002. Control of goal-directed and stimulus-driven attention in the brain. Nat. Rev. Neurosci. 3 (3), 201.

Curtis, C.E., 2006. Prefrontal and parietal contributions to spatial working memory. Neuroscience 139 (1), 173–180.

Eippert, F., et al., 2007. Regulation of emotional responses elicited by threat-related stimuli. Hum. Brain Mapp. 28 (5), 409–423.

Frank, D.W., et al., 2014. Emotion regulation: quantitative meta-analysis of functional activation and deactivation. Neurosci. Biobehav. Rev. 45, 202.

Goulas, A., Uylings, H.B., Stiers, P., 2012. Unravelling the intrinsic functional organization of the human lateral frontal cortex: a parcellation scheme based on resting state fMRI. J. Neurosci. Official J. Soc. Neurosci. 32 (30), 10238.

Guevara, M., et al., 2017. Reproducibility of superficial white matter tracts using diffusion-weighted imaging tractography. NeuroImage 147, 703.

Hopfinger, J.B., Buonocore, M.H., Mangun, G.R., 2000. The neural mechanisms of top-down attentional control. Nat. Neurosci. 3 (3), 284.

Kringelbach, M.L., Rolls, E.T., 2004. The functional neuroanatomy of the human orbitofrontal cortex: evidence from neuroimaging and neuropsychology. Prog. Neurobiol. 72 (5), 341.

Kujawa, A., et al., 2015. Prefrontal Reactivity to Social Signals of Threat as a Predictor of Treatment Response in anxious Youth. Neuropsychopharmacol. Offic. Publ. Am. Coll. Neuropsychopharmacol. 41 (8), 1983.

Leemans, A., Jones, D.K., 2009. The B-matrix must be rotated when correcting for subject motion in DTI data. Magn. Reson. Med. 61 (6), 1336–1349.

Liu, M., et al., 2016. The superficial white matter in temporal lobe epilepsy: a key link between structural and functional network disruptions. Brain A J. Neurol. (139), 2431 Pt 9.

Mahon, K., Burdick, K.E., Szeszko, P.R., 2010. A role for white matter abnormalities in the pathophysiology of bipolar disorder. Neurosci. Biobehav. Rev. 34 (4), 533–554.

Matsuo, K., et al., 2007. Prefrontal hyperactivation during working memory task in untreated individuals with major depressive disorder. Mol. Psychiatry 12 (2), 158.

Matsuo, K., et al., 2009. Anterior cingulate volumes associated with trait impulsivity in individuals with bipolar disorder. Bipolar Disord. 11 (6), 628–636.

Morawetz, C., et al., 2016. Changes in Effective Connectivity between Dorsal and Ventral Prefrontal Regions Moderate Emotion Regulation. Cereb. Cortex(5).

Nazeri, A., et al., 2013. Alterations of Superficial White Matter in Schizophrenia and Relationship to Cognitive Performance. Neuropsychopharmacol. Offic. Publ. Am. Coll. Neuropsychopharmacol. 38 (10), 1954.

Nazeri, A., et al., 2015. Superficial white matter as a novel substrate of age-related cognitive decline. Neurobiol. Aging 36 (6), 2094–2106.

Nie, J., et al., 2012. Axonal fiber terminations concentrate on gyri. Cereb. Cortex 22 (12), 2831.

Niendam, T.A., et al., 2012. Meta-analytic evidence for a superordinate cognitive control network subserving diverse executive functions. Cogn. Affect. Behav. Neurosci. 12 (2), 241–268.

Oishi, K., et al., 2008. Human brain white matter atlas: identification and assignment of common anatomical structures in superficial white matter. NeuroImage 43 (3), 447.

Phillips, M.L., Swartz, H.A., 2014. A critical appraisal of neuroimaging studies of bipolar disorder: toward a new conceptualization of underlying neural circuitry and a road map for future research. Am. J. Psychiatr. 171 (8), 829.

Phillips, M.L., Ladouceur, C.D., Drevets, W.C., 2008. A neural model of voluntary and automatic emotion regulation: implications for understanding the pathophysiology and neurodevelopment of bipolar disorder. Mol. Psychiatry 13 (9), 829 (833).

Picópérez, M., et al., 2017. Emotion regulation in mood and anxiety disorders: a meta-analysis of fMRI cognitive reappraisal studies. Prog. Neuro-Psychopharmacol. Biol. Psychiatry 79, 96–104.

Reveley, C., et al., 2015. Superficial white matter fiber systems impede detection of long-range cortical connections in diffusion MR tractography. Proc. Natl. Acad. Sci. U. S. A. 112 (21), E2820.

Rosenbloom, M.H., Schmahmann, J.D., Price, B.H., 2012. The functional neuroanatomy of decision-making. J. Neuropsychiatr. Clin. Neurosci. 24 (3), 266.

Saarimäki, H., et al., 2016. Discrete Neural Signatures of Basic Emotions. Cereb. Cortex 26 (6), 2563.

Smith, S.M., Nichols, T.E., 2009. Threshold-free cluster enhancement: addressing problems of smoothing, threshold dependence and localisation in cluster inference. NeuroImage 44 (1), 83.

Smith, S.M., et al., 2006. Tract-based spatial statistics: voxelwise analysis of multi-subject diffusion data. NeuroImage 31 (4), 1487–1505.

Townsend, J., Altshuler, L.L., 2012. Emotion processing and regulation in bipolar disorder: a review. Bipolar Disord. 14 (4), 326–339.

Townsend, J.D., et al., 2013. Frontal-amygdala connectivity alterations during emotion down-regulation in bipolar I disorder. Biol. Psychiatry 73 (2), 127–135.

Treadway, M.T., et al., 2009. Early adverse events, HPA activity and Rostral Anterior Cingulate volume in MDD. PLoS One 4 (3), e4887.

Wager, T.D., Smith, E.E., 2003. Neuroimaging studies of working memory: a meta-analysis. Cogn. Affect. Behav. Neurosci. 3 (4), 255–274.

Wagner, G., et al., 2006. Cortical inefficiency in patients with unipolar depression: an event-related FMRI study with the Stroop task. Biol. Psychiatry 59 (10), 958–965.

Wakana, S., et al., 2007. Reproducibility of quantitative tractography methods applied to cerebral white matter. NeuroImage 36 (3), 630–644.

Whisman, M.A., et al., 1989. A structured interview guide for the Hamilton Depression Rating Scale for Depression. Psychol. Assess. 1 (3), 238–241.

Winkler, A.M., et al., 2014. Permutation inference for the general linear model. NeuroImage 92 (100), 381.

Young, R.C., et al., 1978. A rating scale for mania: reliability, validity and sensitivity. Br. J. Psychiatry J. Ment. Sci. 133 (5), 429.

Zilverstand, A., M.A. Parvaz, and R.Z. Goldstein, Neuroimaging cognitive reappraisal in clinical populations to define neural targets for enhancing emotion regulation. A systematic review. NeuroImage, 2016. 151.